Excess Specific Heat in Evaporated Amorphous Silicon

D. R. Queen,[1,*] X. Liu,[2] J. Karel,[3] T. H. Metcalf,[2] and F. Hellman[1,3]
[1]*Department of Physics, University of California, Berkeley, Berkeley, California 94720, USA*
[2]*Naval Research Laboratory, Washington, DC 20375, USA*
[3]*Department of Materials Science and Engineering, University of California, Berkeley, Berkeley, California 94720, USA*

(Received 3 May 2012; revised manuscript received 2 January 2013; published 28 March 2013)

The specific heat C of e-beam evaporated amorphous silicon (a-Si) thin films prepared at various growth temperatures T_S and thicknesses t was measured from 2 to 300 K, along with sound velocity v, shear modulus G, density n_{Si}, and Raman spectra. Increasing T_S results in a more ordered amorphous network with increases in n_{Si}, v, G, and a decrease in bond angle disorder. Below 20 K, an excess C is seen in films with less than full density where it is typical of an amorphous solid, with both a linear term characteristic of two-level systems (TLS) and an additional (non-Debye) T^3 contribution. The excess C is found to be independent of the elastic properties but to depend strongly on density. The density dependence suggests that low energy glassy excitations can form in a-Si but only in microvoids or low density regions and are not intrinsic to the amorphous silicon network. A correlation is found between the density of TLS n_0 and the excess T^3 specific heat c_{ex} suggesting that they have a common origin.

DOI: 10.1103/PhysRevLett.110.135901 PACS numbers: 65.60.+a, 61.43.Dq, 63.50.−x

The low temperature thermal properties of amorphous solids are known to be markedly different from their crystalline counterparts due to low energy excitations not typically found in crystalline materials [1]. These excitations result in an increase in the low temperature heat capacity and cause strong scattering of phonons and elastic waves. Many of these properties are explained by the two-level systems (TLS) model that assumes single atoms or groups of atoms can have energetically similar configurations and, at low temperature where thermal activation over the energy barrier separating configurations is not possible, a finite tunneling probability exists which splits the ground state energy [2,3]. While the TLS model explains a wide range of experimental results, it offers little insight into the physical nature of the tunneling entities themselves. Despite 40 years of active research several open questions remain: Why are TLS found with roughly the same density in most amorphous solids? Are these excitations intrinsic to the amorphous state? Do TLS form in tetrahedral bonded materials like a-Si and a-Ge? Interest has been renewed in understanding the origin of TLS as they cause decoherence in solid state qubits [4] and noise in superconducting resonators [5].

Specific heat C is a sensitive measure of these low energy excitations. For a dielectric, amorphous solid at low temperature,

$$C = c_1 T + c_3 T^3. \tag{1}$$

c_1 is due to TLS and is calculated in the TLS model [6] as

$$c_1 = \frac{\pi^2}{6} k_B^2 n_0 \frac{N_A}{n_{\mathrm{Si}}}, \tag{2}$$

where n_0 is the density of TLS, n_{Si} the atomic density, k_B Boltzmann's constant, and N_A Avogadro's number.

$$c_3 = c_D + c_{\mathrm{ex}}, \tag{3}$$

where c_D is the Debye specific heat due to phonons and is calculated from the sound velocity. Typically, $c_3 > c_D$ and we define c_{ex} as the excess T^3 term. c_{ex} is not part of the TLS model and is thought to result from nonpropagating harmonic modes [7]. In most amorphous solids, $n_0 \sim 10^{45}$–10^{46} $\mathrm{J^{-1}\,m^{-3}}$ while $c_{\mathrm{ex}} \approx 1$–$10 \times 10^{-5}$ $\mathrm{J\,mol^{-1}\,K^{-4}}$ and within an order of magnitude of c_D [7]. The narrow range of n_0 found for a wide variety of glasses has led to speculation that n_0 is a universal property of glasses. It is not clear how the states responsible for n_0 and c_{ex} are related.

Phillips suggested that TLS form in materials that have an open structure with low coordination sites; tetrahedrally bonded materials, like a-Si, are then overconstrained and TLS should not occur [2]. Liquid silicon cannot be quenched fast enough to form a glass but a-Si can be prepared by thin film deposition techniques. The difficulty in preparing the several milligrams of material needed for a conventional calorimeter has meant that few C results are found in the literature. Unlike vitreous silica where n_0 changes little between samples [6], conflicting results are reported for a-Si ranging from $n_0 \sim 0$ [8,9] to $n_0 = 10^{47}$ $\mathrm{J^{-1}\,m^{-3}}$ [10]. Other tetrahedrally bonded materials similarly show a range of behaviors with TLS found in a-$\mathrm{CdGeAs_2}$ [11] but not in a-Ge [12,13]. Recently, hydrogenated amorphous silicon (a-Si:H) has been prepared with a TLS density that is far below the "universal" range but it is not clear if hydrogen is required to suppress TLS in a-Si [14].

In this Letter, we present specific heat $C(T)$ measurements from 2–300 K for e-beam evaporated a-Si films grown at various temperatures T_S and thicknesses t on membrane-based nanocalorimeters [15]. The low background heat

TABLE I. Summary of data: sample number, growth temperature T_S, sample thickness t, silicon number density n_{Si} (for crystalline Si $n_{\mathrm{Si}} = 5.00 \times 10^{22}\ \mathrm{cm}^{-3}$), dangling bond density n_{ESR}, longitudinal sound velocity v_l, transverse sound velocity v_t, and shear modulus G. Values in parenthesis were not measured. θ_D is the Debye temperature calculated from v_l and v_t with c_D the corresponding T^3 specific heat. c_1 and c_3 are from fits to C at low T using Eq. (1). n_0 is the density of TLS from c_1. $c_{\mathrm{ex}} = c_3 - c_D$ is the excess T^3 specific heat.

Sample	T_S °C	t nm	n_{Si} $\times 10^{22}$ cm^{-3}	n_{ESR} $\times 10^{18}$ cm^{-3}	G GPa	v_l nm/ps	v_t nm/ps	θ_D K	c_D $\times 10^{-5}$ J/mol K^4	c_1 $\times 10^{-4}$ J/mol K^2	c_3 $\times 10^{-5}$ J/mol K^4	n_0 $\times 10^{46}$ $\mathrm{J}^{-1}\ \mathrm{m}^{-3}$	c_{ex} $\times 10^{-5}$ J/mol K^4
1	45	112	4.14	6.6	...	8.04	(4.11)	476	1.8	16	5.9	36	4.1
2	45	278	4.33	6.0	35	7.38	4.11	479	1.8	1.9	3.9	4.6	2.1
3	200	153	4.26	6.7	...	8.49	(4.75)	550	1.2	8.0	5.4	1.8	4.2
4	200	319	4.36	5.8	46	8.80	4.75	560	1.1	1.8	2.2	4.3	1.1
5	400	310	4.71	...	58	8.66	5.13	611	0.9	0.1	1.2	0.2	0.4
Ref. [9]	45	415	4.68	~10	...	7.51	...	485	1.7	0	1.7	0	0

capacity of the nanocalorimeter allows $C(T)$ measurements on thin films over a wide temperature range. The sound velocity, and thus c_D, is shown to increase with T_S while both n_0 and c_{ex} vary widely, even for films with the same sound velocity, indicating that the low energy excitations are independent of the elastic properties of the material. We show here that the variability of n_0 and c_{ex} is explained by a dependence on n_{Si}, and only indirectly on T_S, suggesting that TLS and nonpropagating harmonic modes in a-Si occur in the low density regions of the film and are not associated with disorder in the tetrahedrally bonded network. Further, we show that these two phenomena are linked and likely have a common structural origin.

a-Si thin films were prepared by e-beam evaporation from a high purity Si source with a background pressure below 10^{-8} Torr and a growth rate of 0.05–0.1 nm/s. Growth temperature T_S was varied from 45–400 °C. After evaporation of the a-Si onto the nanocalorimeters, a 20 nm a-AlO$_x$ diffusion barrier was sputtered onto the sample followed by a 30 nm thermally evaporated Cu conduction layer used to provide thermal uniformity.

Film thickness t was measured on films grown on neighboring substrates using a profilometer with an error of 1%–4% depending on film thickness. The uncertainty in film thickness is the dominant source of error in all measurements except at low T where the heat capacity of some samples was less than 10% of the total measured heat capacity; in that case random measurement error dominates. Atomic densities n_{Si} were determined from Rutherford backscattering (RBS) and are shown in Table I. Thinner films and those grown at lower T_S have lower n_{Si}. Oxygen resonant RBS showed a thin surface oxide (1–2 nm) on all films plus a small amount of oxygen (1–5 at. %) throughout the lower density films. The distribution of oxygen is consistent with diffusion into the film after deposition. n_{Si} was also measured for the a-Si sample from Ref. [9].

High-resolution cross-sectional transmission electron microscopy (TEM), as well as electron and x-ray diffraction, showed that the films were fully amorphous with no evidence for nanocrystals or lattice fringes. Low magnification TEM showed a columnar growth structure commonly seen in evaporated films with larger grains for higher T_S films. Raman scattering spectra were measured using the 514.5 nm line of an Ar ion laser and a Jobin-Yvon U-1000 double grating monochromator. See the Supplemental Material [16] for TEM images and Raman spectra. Electron spin resonance (ESR) measurements give dangling bond densities $n_{\mathrm{ESR}} \sim$ 6–7 $\times 10^{18}\ \mathrm{cm}^{-3}$ with gyromagnetic ratio $g = 2.0055$ as is typical for isolated, neutral dangling bonds in a-Si [17]. n_{ESR} decreases sightly as n_{Si} increases as expected [18]. Oxidation is known to decrease n_{ESR} [17].

Longitudinal sound velocities v_l were measured using an ultrasonic pump-probe technique [19]. Films were also grown on single crystal double paddle oscillators for measurement of the internal friction and shear modulus $G = \rho v_t^2$ where ρ is the mass density and v_t is the transverse sound velocity [20]. Heat capacity measurements were made from 2–300 K using a thin film nanocalorimeter [15,21,22].

Figure 1 shows C/T^3 for a-Si films grown at various T_S and t along with the film from Ref. [9], where C was found to be close to the Debye value. The dashed horizontal lines are the Debye specific heats $c_D T^3 = 12\pi^4/5N_A k_B (T/\theta_D)^3$ calculated from the sound velocity using the Debye temperature $\theta_D = \hbar v_D / k_B (6\pi^2 n_{Si})^{1/3}$ where $v_D = [\frac{1}{3} v_l^{-3} + \frac{2}{3} v_t^{-3}]^{-1/3}$. For thinner films where v_t was not measured, v_t for the same T_S sample was used since no dependence on t was found in v_l (see inset Fig. 1). The linear C due to TLS appears as an upturn at low T and the $c_{\mathrm{ex}} T^3$ term leads to the increase above c_D at intermediate temperatures. The maximum in C/T^3 in crystalline solids, such as Si (c-Si), is due to a peak in the phonon density of states from transverse acoustic phonons at the Brillouin-zone boundary. Similar modes are thought to be responsible for the maximum in amorphous solids [23] which is often called the boson peak after a similar feature found in optical measurements [6,24]. The boson peak in a-Si is visible in Fig. 1 (particularly for films with small excess C) at $T_{\max} \sim 35$ K, which is indicated by the vertical arrow, and does not depend

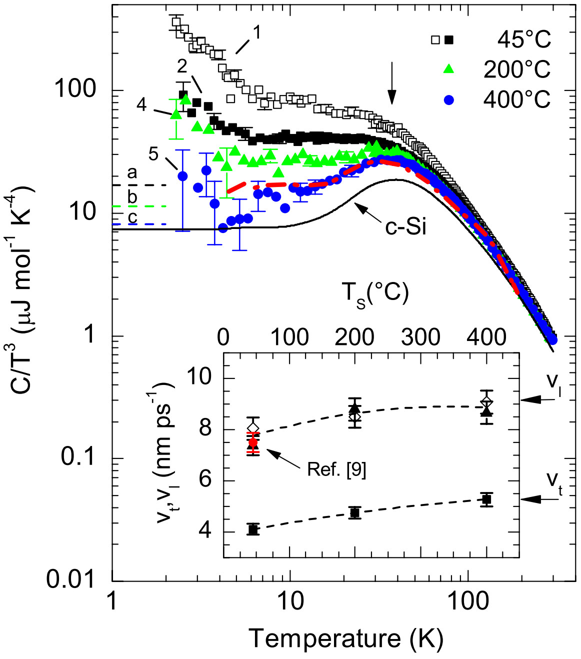

FIG. 1 (color online). Specific heat of a-Si plotted as C/T^3 versus T for several T_S and t. (Samples identified by number.) Data for sample 3 are close to sample 1 and are not shown. Representative error bars are shown for clarity. Horizontal dashed lines show low T Debye specific heat for $\theta_D =$ (a) 479, (b) 560, and (c) 611 K (corresponding or near to samples 1–5). Excess C visible as low T upturn in C, which is well above C_D. Data for a-Si from Ref. [9] (red dash-dotted line) and crystalline silicon (black solid line) [41]. $\theta_D = 645$ K for crystalline silicon. Vertical arrow identifies location of the boson peak. Inset: v_t (solid squares) for thick and v_l for thick (solid triangles) and thin (open diamonds) films vs T_S. v_l from Ref. [9] (solid diamond). Arrows indicate polycrystalline average: $v_l(v_t) = 9.14(5.28)$ nm/ps. Lines are a guide to the eye.

significantly on T_S. The peak seen in the Raman spectra also shows no dependence on T_S [25]. At room temperature, C of all films match to within error in t indicating that errors in $C(T)$ from uncertainty in t or n_{Si} are small. At low T, thinner films (#1 and #3), show greater C enhancement than thicker films (#2 and #4) grown at the same T_S; we will show below that this is associated with reduced n_{Si} in the thinner films. C is independent of the oxygen content in the films. Measurements in 4 and 8 T magnetic fields showed no field dependence indicating the electronic states of the dangling bonds are not responsible for the increase in C [13].

The Fig. 1 inset shows that v_l and v_t increase with T_S (and are independent of t) as is also found in a-Si:H [26]. Correspondingly, the linewidth of the Raman peak at 480 cm^{-1} decreases with increasing T_S indicating a decrease in bond angle disorder [25,27]. Thus increasing T_S reduces the overall disorder in the film and results in an increase in the elastic properties which approach the crystalline values [26,28].

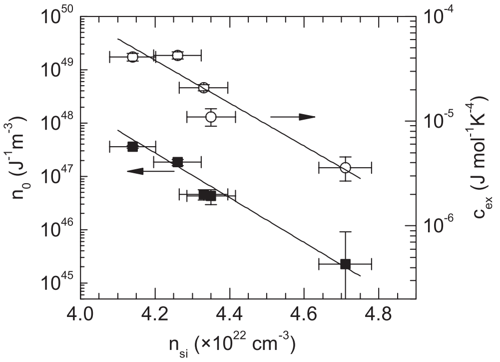

FIG. 2. n_0 (solid squares) and $c_{\mathrm{ex}} = c_3 - c_D$ (open circles) as a function of n_{Si}. The lines are a guide to the eye.

C data below 12 K have been fit to Eq. (1) to determine the glassy contribution to C and, thus, n_0 and c_{ex}. The results are summarized in Table I. Unlike the elastic properties where only T_S is important, n_0 and c_{ex} are not simply dependent on T_S (or c_D), but instead depend on n_{Si}, as shown in Fig. 2. The 400 °C film and the 45 °C film from Ref. [9] have Debye-like C with small n_0 and c_{ex}. Both films have $n_{\mathrm{Si}} \sim 94\%$ of the crystalline value. Films grown at other T_S and of different t have somewhat lower n_{Si} (83%–87% of the crystalline value) and significant n_0 and c_{ex}. The dependence of n_0 and c_{ex} on n_{Si} suggests that low energy excitations occur either in voids or other low density regions in the film and are independent of the elastic properties which are determined by the average local structure.

Figure 2 also suggests a strong correlation between n_0 and c_{ex}, plotted in Fig. 3. This correlation is not addressed in the TLS model but has previously been suggested. A relationship was found between c_1 and c_3 for several glasses when the terms were weighted by θ_D [11] and a study of TLS and rigidity percolation in a-As$_x$Se$_{1-x}$ also found a correlation between c_1 and c_3 where both terms depended on density [29,30]. Comparison of amorphous solids with different chemical compositions has made it

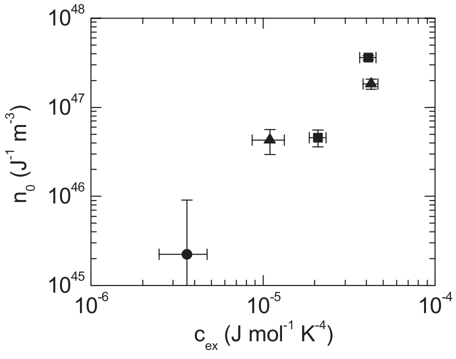

FIG. 3. n_0 vs c_{ex} determined from fits to C as described in the text. Data points identified by growth temperature 45 °C (solid squares), 200 °C (solid triangles), and 400 °C (solid circle).

difficult to interpret this correlation as the elastic constants differ and the chemical environment of the TLS is unknown. We find that the elastic properties do not affect TLS formation even though TLS do interact strongly with elastic waves as observed in thermal conductivity and acoustic attenuation [31]. Our results suggest that the low atomic density environment of the tunneling entities differs from the average environment in a-Si which is measured by techniques like Raman scattering.

The microstructure of a-Si is known to be sensitive to the growth process and both local structure and voids affect n_{Si} [32]. For evaporated films, the increase in n_{Si} with T_S is likely the result of increased surface mobility during the growth process resulting in larger grains and reduced bond angle disorder. An increase in n_{Si} with t is also observed and its origin is less clear. RBS shows that n_{Si} is constant through the thickness of the film and TEM shows that the columnar structure is uniform throughout the film. It is not clear what growth mechanism leads to an increase in n_{Si} with t without a density gradient, but this is not uncommon in films. Most importantly, a model considering excess C as associated with a gradient of n_{Si} that increases with t is inconsistent with the data since the total heat capacity at low T of thinner films (in J/K, not normalized by film volume) is larger than that of thicker films.

It has been suggested that TLS will form in voids [33] and low density regions frozen in at the glass transition [34]. This appears to be true in network glasses such as a-Ge [35], a-$\mathrm{As}_x\mathrm{Se}_{1-x}$ [29], and a-Si. Two-state system dynamics have recently been reported for clusters of 4–6 atoms on a-Si surfaces [36]. It seems reasonable that similar groups of Si atoms on the surfaces of voids form the tunneling entities that give rise to n_0.

It is clear from Figs. 2 and 3 that the excitations giving rise to n_0 are closely related to the harmonic modes responsible for c_{ex}. Inelastic neutron scattering [37] and molecular dynamics simulations [38] both associate an increase in the vibrational density of states in a-Si to modes localized near voids. These modes are absent in simulations of full density networks [39,40], supporting our interpretation that the excess C (both n_0 and c_{ex}) in a-Si results from excitations forming in low density regions or voids.

We note that a soft-potential model (SPM) depending on n_{Si} and v_D has been proposed to explain TLS and the features at higher T. However, that model does not seem to apply to this system as our results are independent of v_D and do not show the appropriate dependence on n_{Si}. Also, our data do not fit well to the SPM which includes an additional c_5T^5 term to account for the low temperature shoulder of the boson peak; we find $c_5 \sim 0$, consistent with the boson peak being independent of sample.

In summary, we have shown that low energy excitations do occur in a-Si and that they are independent of the elastic properties. Increasing T_S leads to an increase in sound velocity and θ_D that is associated with a decrease in bond angle disorder. The excess C at low T due to glassy excitations is largest in films with low density while high density films have C comparable to c_D. We have shown clear quantitative correlation between the linear TLS density n_0 and the non-Debye excess T^3 heat capacity c_{ex} suggesting a common origin for both. These results show that glassy excitations do occur in a-Si, a monatomic tetrahedrally bonded material, but are not an intrinsic result of the disordered a-Si network and thus not universal. We suggest that tunneling entities in a-Si are groups of atoms on the surfaces of voids that form in conjunction with localized vibrational modes.

We thank G. T. Hohensee and D. G. Cahill for sound velocity, K. M. Yu for assistance with RBS, D. J. Smith for TEM, J. W. Ager for assistance with Raman, and D. Bobela for ESR. C_P measurements supported by NSF DMR-0907724, film growth and nanocalorimeter development supported by the U.S. Department of Energy DE-AC02-05CH11231, and internal friction measurements supported by the Office of Naval Research.

---

[*] Current address: Naval Research Laboratory, Washington, DC 20375, USA.

[1] R. C. Zeller and R. O. Pohl, Phys. Rev. B **4**, 2029 (1971).
[2] W. A. Phillips, J. Low Temp. Phys. **7**, 351 (1972).
[3] P. W. Anderson, B. I. Halperin, and C. M. Varma, Philos. Mag. **25**, 1 (1972).
[4] J. M. Martinis, K. B. Cooper, R. McDermott, M. Steffen, M. Ansmann, K. D. Osborn, K. Cicak, S. Oh, D. P. Pappas, R. W. Simmonds, and C. C. Yu, Phys. Rev. Lett. **95**, 210503 (2005).
[5] J. Gao, J. Zmuidzinas, B. A. Mazin, H. G. LeDuc, and P. K. Day, Appl. Phys. Lett. **90**, 102507 (2007).
[6] *Amorphous Solids Low Temperature Properties*, edited by W. A. Phillips (Springer, New York, 1981).
[7] R. B. Stephens, Phys. Rev. B **8**, 2896 (1973).
[8] M. Mertig, G. Pompe, and E. Hegenbarth, Solid State Commun. **49**, 369 (1984).
[9] B. L. Zink, R. Pietri, and F. Hellman, Phys. Rev. Lett. **96**, 055902 (2006).
[10] J. E. Graebner, B. Golding, L. C. Allen, J. C. Knights, and D. K. Biegelsen, Phys. Rev. B **29**, 3744 (1984).
[11] D. G. Cahill and R. O. Pohl, Phys. Rev. B **37**, 8773 (1988).
[12] H. v. Löhneysen and H. J. Schink, Phys. Rev. Lett. **48**, 1121 (1982).
[13] R. van den Berg, H. Löhneysen, and H. J. Schink, J. Non-Cryst. Solids **77**, 1339 (1985).
[14] X. Liu, B. E. White, R. O. Pohl, E. Iwanizcko, K. M. Jones, A. H. Mahan, B. N. Nelson, R. S. Crandall, and S. Veprek, Phys. Rev. Lett. **78**, 4418 (1997).
[15] D. R. Queen and F. Hellman, Rev. Sci. Instrum. **80**, 063901 (2009).
[16] See Supplemental Material at http://link.aps.org/supplemental/10.1103/PhysRevLett.110.135901 for TEM images, which show the films are amorphous and have a

columnar growth structure, and Raman scattering spectra with the resulting bond angle disorder.

[17] P. A. Thomas, M. H. Brodsky, D. Kaplan, and D. Lepine, Phys. Rev. B **18**, 3059 (1978).

[18] M. H. Brodsky, D. Kaplan, and J. F. Ziegler, Appl. Phys. Lett. **21**, 305 (1972).

[19] T. Lee, K. Ohmori, C. S. Shin, D. G. Cahill, I. Petrov, and J. E. Greene, Phys. Rev. B **71**, 144106 (2005).

[20] X. Liu, T. H. Metcalf, P. Mosaner, and A. Miotello, Phys. Rev. B **71**, 155419 (2005).

[21] D. W. Denlinger, E. N. Abarra, K. Allen, P. W. Rooney, M. T. Messer, S. K. Watson, and F. Hellman, Rev. Sci. Instrum. **65**, 946 (1994).

[22] B. Revaz, B. L. Zink, and F. Hellman, Thermochim. Acta **432**, 158 (2005).

[23] X. Liu and H. V. Löhneysen, Europhys. Lett. **33**, 617 (1996).

[24] J. S. Lannin, L. J. Pilione, S. T. Kshirsagar, R. Messier, and R. C. Ross, Phys. Rev. B **26**, 3506 (1982).

[25] D. R. Queen, Ph.D. thesis, University of California, Berkeley, 2011, p. 34.

[26] H. S. Yang, D. G. Cahill, X. Liu, J. L. Feldman, R. S. Crandall, B. A. Sperling, and J. R. Abelson, Phys. Rev. B **81**, 104203 (2010).

[27] D. Beeman, R. Tsu, and M. F. Thorpe, Phys. Rev. B **32**, 874 (1985).

[28] M. A. Hopcroft, W. D. Nix, and T. W. Kenny, J. Microelectromech. Syst. **19**, 229 (2010).

[29] O. Brand and H. Löhneysen, Europhys. Lett. **16**, 455 (1991).

[30] A. Feltz, H. Aust, and A. Blayer, J. Non-Cryst. Solids **55**, 179 (1983).

[31] R. O. Pohl, X. Liu, and T. E, Rev. Mod. Phys. **74**, 991 (2002).

[32] R. Street, *Hydrogenated Amorphous Silicon* (Cambridge University Press, Cambridge, England, 1991).

[33] J. C. Phillips, Phys. Rev. B **24**, 1744 (1981).

[34] M. H. Cohen and G. S. Grest, Phys. Rev. Lett. **45**, 1271 (1980).

[35] J. E. Graebner and L. C. Allen, Phys. Rev. B **29**, 5626 (1984).

[36] S. Ashtekar, G. Scott, J. Lyding, and M. Gruebele, Phys. Rev. Lett. **106**, 235501 (2011).

[37] W. A. Kamitakahara, C. M. Soukoulis, H. R. Shanks, U. Buchenau, and G. S. Grest, Phys. Rev. B **36**, 6539 (1987).

[38] S. M. Nakhmanson and D. A. Drabold, Phys. Rev. B **61**, 5376 (2000).

[39] J. L. Feldman, M. D. Kluge, P. B. Allen, and F. Wooten, Phys. Rev. B **48**, 12589 (1993).

[40] J. L. Feldman, P. B. Allen, and S. R. Bickham, Phys. Rev. B **59**, 3551 (1999).

[41] Y. Touloukian, *Thermophysical Properties of Matter* (Plenum, New York, 1970), Vol. 4.